ISSN 1061-8309, Russian Journal of Nondestructive Testing, 2017, Vol. 53, No. 10, pp. 700–706. © Pleiades Publishing, Ltd., 2017.
Original Russian Text © E.S. Gorkunov, S.M. Zadvorkin, L.S. Goruleva, 2017, published in Defektoskopiya, 2017, No. 10, pp. 26–33.

MAGNETIC METHODS

Relationship Between the Structure and Physical-Mechanical Properties of U8A Steel Subjected to Cold Plastic Deformation by Hydrostatic Extrusion

E. S. Gorkunov*, S. M. Zadvorkin, and L. S. Goruleva*****

Institute of Engineering Science, Ural Branch, Russian Academy of Sciences, Yekaterinburg, 620049 Russia

**e-mail: ges@imach.uran.ru*

***e-mail: zadvorkin@imach.uran.ru*

****e-mail: sherlarisa@yandex.ru*

Received May 5, 2017

Abstract—The structure and physical-mechanical properties of U8A high-carbon steel subjected to cold plastic deformation by hydrostatic extrusion have been investigated in a wide range of strain extents. Cold plastic deformation by hydrostatic extrusion has been shown to lead to the dispersion of the structure of U8A high-carbon steel. As the degree of true deformation increases, the ultimate strength and conventional yield limit of U8A steel monotonically grow by 2 and 3.6 times, respectively. Such parameters as coercive force, the number of jumps in magnetic Barkhausen noises, maximum magnetic permeability, residual induction, and the speed of elastic waves are more sensitive to changes in the dislocation density than in the dispersion of the grain and subgrain structure of extruded U8A steel. It has been established that at least two informative testing parameters are needed for nondestructive evaluation of the level of strength properties in extruded U8A steel. Those are coercive force (or maximum magnetic permeability, residual induction, the number of Barkhausen jumps, the speed of elastic waves) for a true deformation of up to 1.62 and the root-mean-square voltage of magnetic Barkhausen noises for true deformations above 1.62.

Keywords: hydrostatic extrusion, high-carbon steel, structure, physical-mechanical properties

DOI: 10.1134/S1061830917100059

INTRODUCTION

Increasing the strength properties of materials by severe plastic deformation (SPD) is now gaining popularity. Strength properties improve primarily due to the dispersion of structure and increase in dislocation density [1–5]. In [6], it was shown that equal channel angular pressing (ECAP) can be used to double the ultimate strength and conventional yield limit of economically doped 09G2S. A peculiarity of such an SPD method as hydrostatic extrusion (hydraulic forging) is the possibility for cold plastic deformation, a method that is most effective when raising the strength by means of the dispersion of structure and the increase of dislocation density even in brittle materials (for example, high-carbon steels) [7]. Hydrostatic extrusion can be used for cold deformation of brittle materials in a wide range of strain extents. In addition, this method of deformation hinders formation of cracks in the material being processed.

The influence of SPD, including by hydrostatic extrusion, on the structure and mechanical properties of pure metals, alloys, and steels has been described in great detail in the literature [8, 9]. Much less emphasis has been placed on studying the physical characteristics of SPD-strengthened materials. Such studies are necessary for the development of nondestructive physical methods of testing the condition of these materials. The use of magnetic methods of nondestructive testing helps to significantly optimize the production process while improving the specs of the produce (see, for example, [10–12]).

In this paper, the structure and physical-mechanical properties of U8A eutectoid steel subjected to severe plastic deformation action by hydrostatic extrusion at room temperature were examined.

SAMPLES AND RESEARCH METHODS

U8A (0.8 mass % C) hot-rolled rod iron of commercial heat in as received state was used as the material for research. Plastic deformation of rods by hydrostatic extrusion was performed at room temperature following the sequential root ∅18 mm → ∅12 mm → ∅10 mm → ∅8 mm → ∅6 mm.[1] The doubled entry cone angle of the die mouth was 30°—35°. Such a large die-mouth angle may lead to formation of cracks in the material being processed [13]. However, the microscopic research of extrudates did not reveal any cracks in them. As a result, four extrudates were obtained with the true deformation extents $e = 0.81$, 1.17, 1.62, and 2.19, respectively, with the extent being calculated [14] by the formula

$$e = 2\ln(d_0/d_i),$$

where d_0 is the rod diameter in the initial state and d_i is the diameter of the rod after the i-th compaction pass.

The microstructure of U8A steel in the initial and post-extrusion conditions was performed on longitudinal thin sections by electron backscattered diffraction (EBSD) technique using an MIRA 3LMH scanning electron microscope with a scanning pitch of 100 nm.[2] The criterion for selecting the scanning pitch was the average size of grains in the extrudate with the maximum true deformation, which, according to the data of a preliminary microscopic examination, was approximately 350 nm. When analyzing the EBSD maps by the CHANNEL 5 software, the sizes of grains and subgrains were calculated. According to [15], any structural elements with a misorientation under 15° were taken to be subgrains, and those with a misorientation over 15° were taken to be grains.

X-ray images of longitudinal and transverse thin sections were employed to determine the presence of a crystallographic texture with a SHIMADZU XRD 7000 diffractometer using the K_α—radiation from a chromium anode. The samples were electropolished prior to X-ray diffraction analysis.

The mechanical properties of steel (ultimate strength σ_u, conventional yield limit $\sigma_{0.2}$, and failure elongation δ) in the initial and post-extrusion states were determined on five-to-one cylindrical headed test bars using an INSTRON 8801 universal testing machine. In addition, the *HRB* hardness was measured. In what follows, we provide data on σ_u, $\sigma_{0.2}$, δ, and *HRB* averaged over the results of testing three samples for each true-deformation value. The error in determining the mechanical characteristics did not exceed 5%.

The magnetic characteristics of samples (coercive force H_c, maximum magnetic permeability μ_{max}, residual magnetic induction B_r, and saturation magnetization M_s) were determined from the initial magnetization curves and major magnetic-hysteresis loops using a Remagraph C-500 magnetic-measurement facility. The sample was magnetized in a permeameter, with the magnetic field of ±60 kA/m applied in the direction of the longer sample axis. The error in determining the mechanical characteristics did not exceed 3%.

Using a MICROSCAN 600 magnetic-Barkhausen-noise (MBN) analyzer, the root-mean-square MBN voltage (U) and the number of Barkhausen jumps (N) were determined with a magnetization reversal frequency of 115 Hz for packs of 10 cycles. The analyzer's attachable transducer was placed in the middle of the sample for the sample magnetization to occur in the direction of the longer sample axis when measuring the MBN parameters. Five series of U and N measurements with transducer reset were taken for each sample, followed by the averaging of the results.

The speed V of elastic waves was measured using a double electromagnetic–acoustic transducer (EMAT) operating in the resonance mode with the use of through-pass sensors. The zero symmetric mode of longitudinal normal elastic waves was employed. The external polarizing constant magnetic field, which was created by an electromagnet and directed along the sample axis, was selected for each sample separately from the maximum of the EMAT-signal amplitude when in resonance. In this case, the error in determining the propagation speed of elastic waves was no more than 2%.

RESULTS AND DISCUSSION

Figure 1 presents the EBSD maps of longitudinal thin sections for some of the samples studied. It can be seen that steel in as received state has the structure of granular pearlite with average grain and subgrain sizes of 20 and 4 μm, respectively. Increase in true deformation gives rise to the dispersion of the material structure so that at $e = 2.19$ the average grain size drops to 0.4 μm, while the average size of the subgrains diminishes to 0.24 μm. It should be noted that for e greater than 1.62 (the extrudate dimeter of less than 8 mm), the

[1] Deformation was carried out in the laboratory of high-pressure physics at the Mikheev Institute of Physics of Metals, Ural Branch, Russian Academy of Sciences.

[2] The research was conducted at the Institute of Metals Superplasticity Problems, Russian Academy of Sciences.

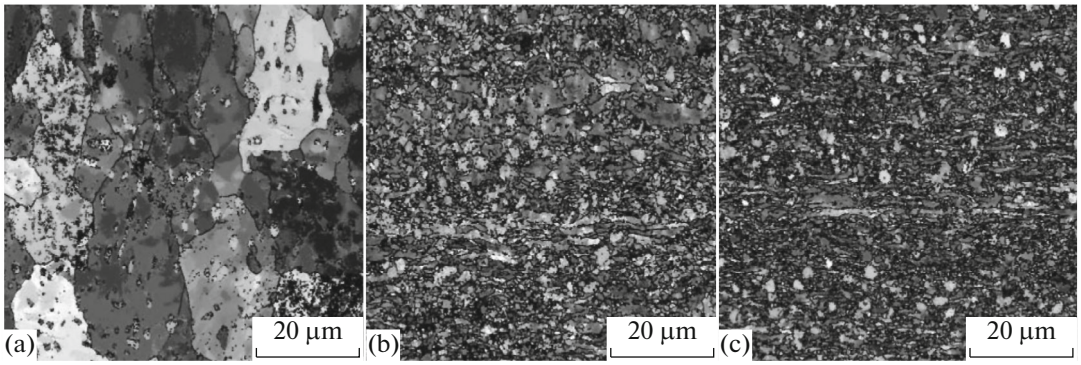

Fig. 1. EBSD maps of the microstructure of U8A steel in the initial and post-extrusion states (longitudinal thin sections): (a) initial state (average grain size 20 μm), (b) true deformation 1.62 (average grain size 1.2 μm), (c) true deformation 2.19 (true grain size 0.4 μm).

structure exhibits a certain amount of nonequiaxed grains that are substantially larger along the axis than in the transverse direction.

It is known [16] that drawing (compaction, uniaxial tension) in metals with BCC structure results in the formation of an axial single-component crystallographic texture of ⟨1 1 0⟩ type. X-ray diffraction examination showed that a similar structure is present in the rods even in the initial state, prior to extrusion: the intensities of X-ray reflexes with the same indices differ two times in the diffraction patterns from the longitudinal and transverse thin sections. After the first compaction pass, the degree of texturization grows, with the ratio of the intensities of diffraction maxima with the same indices reaching 10 times. However, further compaction passes leave the ratio of the intensities of X-ray reflexes intact, i.e., the degree of texturization of the material does not change.

It was demonstrated in [17], where the dislocation structure of the same samples as the ones used in the present paper was studied, that increasing e from 0 to 1.62 (extrudate diameter 8 mm) increases the density of free dislocations from 3×10^{10} to 8×10^{10} cm^{-2}, while at the last extrusion stage (∅8 mm → ∅6 mm) the dislocation density drops to 4×10^{10} cm^{-2}, that is, almost to its value in the initial state. The fact that the density of free dislocations decreases during the last extrusion stage is confirmed by an increase in the size of coherent-scattering domains (those domains in the material that scatter X-rays as an ideal crystal, i.e., flawless domains) as the true-deformation extent grows from 1.62 to 2.19. It was suggested in [17] that decrease of the dislocation density at the last extrusion stage occurs due to the development of continuous dynamic recrystallization.

Metallographic studies showed that extrusion is accompanied by a decrease in the content of cementite in the structure of U8A steel, but carbide particles remain in the structure of the studied samples even for the maximum true-deformation value. Deformational dissolution of cementite in carbon steels has been described by V.M. Schastlivtsev (see, for example, [18]). Studying the saturation magnetization of the samples showed that the value of M_s remains constant to within the error, a fact that indicates the stability of the phase composition of U8A steel.

Figure 2 shows dependences of the physical characteristics of the studied samples on the true deformation. It can be seen that as e increases to 1.62, the coercive force grows linearly almost twofold, the maximum magnetic permeability increases by 1.5 times, and the residual induction goes up by approximately 15%. The propagation speed of elastic waves V and the number N of Barkhausen jumps also varies monotonically within this interval of true deformations (see Fig. 2b). During the last extrusion pass, i.e., when e increases from 1.62 to 2.19, H_c and N decrease, while μ_{max}, B_r, and V increase. Extrema around the true-deformation extent of approximately 1.62 are thus formed on the dependences $H_c(e)$, $N(e)$, $\mu_{max}(e)$, $B_r(e)$, and $V(e)$. Unlike other magnetic parameters, the root-mean-square MBN voltage U behaves differently, namely, the first deformation pass ($e = 0.81$) only slightly affects the value of U, but then, as e increases to 2.19, it monotonically grows by more than 2 times.

The behavior of the magnetic characteristics of extruded U8A steel and the speed of elastic waves in it are primarily influenced by the following factors: the density of free dislocations, the dispersion of structure, fine-dispersed inclusions (cementite particles), and the crystallographic texture and nonequiaxedness of grains. It follows from the model notions about the effect of structural properties on magnetic parameters that the coercive force is proportional to the square root of the dislocation density [19],

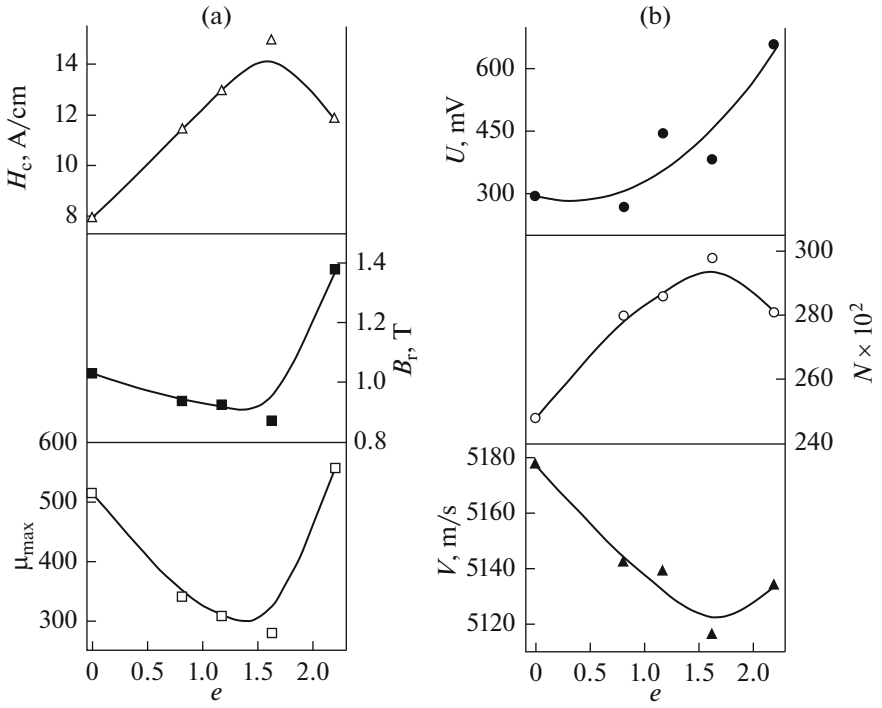

Fig. 2. Dependences of the magnetic characteristics and the propagation speed of elastic waves on the true deformation extent for extruded U8A steel.

inversely proportional to the average grain size and the square root of the subgrain size [20], and proportional to the volume concentration of inclusions [21]. The axial crystallographic texture with the texture axis ⟨110⟩ facilitates magnetization along the extrudate axis as compared to the material with isotropic structure [22]. The nonequiaxedness of grains also promotes magnetization in the grain elongation direction; however, this will have any appreciable effect if the number of such elongated grains is large while the ratio of their sizes in the longitudinal and transverse directions is much greater than 2 [23].

It follows from these peculiarities of the structure of extrudates that the nonequiaxedness of structural elements, the axial crystallographic texture, and the cementite particles do not produce any significant effect on the values of the magnetic parameters being determined and on the propagation speed of elastic waves. A critical role in the formation of the level of physical characteristics is played by such parameters of the structure as the density of free dislocations and the dispersion of structural elements. As mentioned above, the grain and subgrain structure refinement takes place over the entire range of variation of true deformation. This should lead to a monotonical change of the studied physical parameters with the true deformation extent. However, the dependences $H_c(e)$, $N(e)$, $\mu_{max}(e)$, $B_r(e)$, and $V(e)$ exhibit an extremum. The only structural parameter that varies nonmonotonically with e is the density of free dislocations. The maximum in the density of free dislocations is observed at $e = 1.62$, a value that corresponds to the position of the extrema on the dependences $H_c(e)$, $N(e)$, $\mu_{max}(e)$, $B_r(e)$, and $V(e)$. This can be explained by the fact that a decrease in dislocation density at the last stage of extrusion is accompanied by facilitation of magnetization-reversal processes, thus reducing the coercive force and the number of MBN jumps and increasing the maximum magnetic permeability and residual induction. Therefore, we can draw a conclusion that such parameters as H_c, N, μ_{max}, B_r, and V are more sensitive to changes in the density of free dislocations than to changes in the dispersion of the grain and subgrain structure of extruded U8A steel.

Among the physical parameters that we determined, the only one that changed monotonically with true deformation increasing was the root-mean-square MBN voltage. As e grows from 0 to 1.62 due to the dispersion of structure and the increase of the density of free dislocations, i.e., due to an increase in the number of obstacles to the movement of domain walls as samples are magnetized, the number of Barkhausen jumps increases, with the root-mean-square MBN voltage also increasing so that the e.m.f. generated in one jump remains approximately constant. At the last extrusion stage, a certain drop in the number of Barkhausen jumps is observed, while the value of U increases more than over all the previous stages of deformation. This can be explained by a twofold reduction in the density of free dislocations in the mate-

Table 1. Mechanical properties of U8A steel subjected to SPD by hydrostatic extrusion.

True deformations (extrudate diameter)	σ_u, MPa	$\sigma_{0.2}$, MPa	$\sigma_{0.2}/\sigma_u$	δ, %
0 (∅18 mm)	590	325	0.55	14.0
0.81 (∅12 mm)	940	860	0.92	1.5
1.17 (∅10 mm)	1050	960	0.92	1.2
1.62 (∅8 mm)	1170	1120	0.96	0.9
2.19 (∅6 mm)	1330	1170	0.89	1.2

rial as the true deformation extent increases from 1.62 to 2.19. The body of grain thus frees itself from flaws, while the distance that the domain wall covers from one obstacle to another and the speed of movement of domain walls (hence, the generated e.m.f.) increase. This hypothesis is confirmed by the growth of the maximum magnetic permeability at the last extrusion stage.

The mechanical characteristics of the studied samples are listed in Table 1. The strength properties of U8A steel vary monotonically as true deformation grows, viz., the ultimate strength has increased by a factor of 1.5 and the conventional yield limit has grown by 2.6 times even after the first extrusion pass, with both of them growing further during the subsequent passes. The strength properties of the material are influenced by the same structural parameters as the magnetic characteristics. Given the above, one can assume that such structural parameters as the nonequiaxedness of grains and subgrains, the axial crystallographic texture, and the cementite inclusions do not have any significant effect on the strength properties of extruded U8A steel, similar to the physical properties. The other structural parameters that have been considered do produce an immediate effect on the strength characteristics. For example, it is known that the strength characteristics of a material are proportional to the square root of dislocation density [24] and inversely proportional to the square root of the size of structural elements [25]. As the ultimate strength and conventional yield limit do not change monotonically as true deformation grows, a conclusion can be drawn that unlike the magnetic characteristics, the strength characteristics are influenced prevalently by the dispersion of structure, while the density of dislocations plays a secondary role. The growth of $\sigma_{0.2}$ and σ_u is accompanied by a decrease in the failure elongation and an increase in the $\sigma_{0.2}/\sigma_u$ ratio. The latter fact indicates exhaustion of the reserve of strain hardening of materials and increased risk of their brittle failure. The hardness of U8A steel increases after the first hydrostatic compaction pass from *HRB* 85 to *HRB* 100, and then hardly changes.

As the values of σ_u and $\sigma_{0.2}$ of extruded U8A steel change monotonically as the true deformation extent increases (see Table 1), whereas most dependences of physical parameters on e exhibit extrema, it is clear that that there is no one-to-one relationship between strength properties and these physical parameters. Figure 3 shows dependences of the magnetic characteristics and the propagation speed of elastic waves on the ultimate strength of extruded U8A steel. Dependences of the physical characteristics of extruded U8A steel on its conventional yield limit are similar to those shown in Fig. 3. It can be seen that up to $\sigma_u \cong 1170$ MPa (a value that corresponds to the true deformation of 1.62), the coercive force, the maximum magnetic permeability, the residual induction, the number of Barkhausen jumps, and the propagation speed of elastic waves vary unambiguously as the ultimate strength increases. With the further increase of σ_u from 1170 to 1330 MPa (i.e., increase of e from 1.62 to 2.19), the values of H_c and N decrease, while those of μ_{max}, B_r, and V increase. Of the studied physical parameters, the only one that changes monotonically as the ultimate strength increases is the root-mean-square MBN voltage. However, when σ_u increases from 590 to 940 MPa (which corresponds to a cumulative-deformation range of 0—0.81), the root-mean-square MBN voltage changes slightly and only after that, increases by more than 2 times.

These results indicate the necessity of using two-parameter nondestructive testing of the strength properties of U8A steel hardened by severe plastic deformation by hydrostatic extrusion, the parameters being coercive force (or maximum magnetic permeability, residual induction, the propagation speed of elastic waves) up to the true-deformation extent of 1.62 and the root-mean-square voltage of magnetic Barkhausen noises for larger deformations.

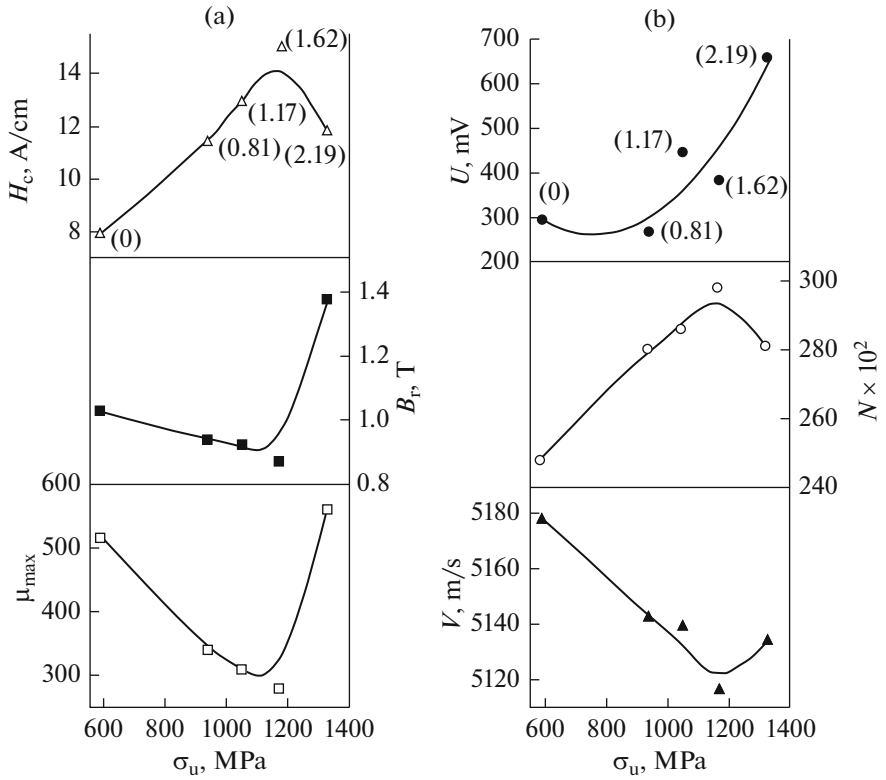

Fig. 3. Relationship of magnetic characteristics and the speed of elastic waves with the ultimate strength of U8A steel (true deformation extents in brackets).

CONCLUSIONS

Cold plastic deformation by hydrostatic extrusion leads to the dispersion of the structure of U8A high-carbon steel, viz., the grain size monotonically decreases from 20, in the initial state, to 0.4 μm for the true-deformation extent of 2.19, while the average size of subgrains reduces from 4 to 0.24 μm.

It has been shown that extrusion results in a monotonical growth of the ultimate strength and conventional yield limit of U8A steel by 2 and 3.6 times, respectively.

It has been established that such parameters as coercive force, the number of magnetic Barkhausen noise jumps, maximum magnetic permeability, residual induction, and the propagation speed of elastic waves are more sensitive to changes in the density of dislocations than to the dispersion of the grain and subgrain structure of extruded U8A steel.

Dependences of the physical parameters on the strength characteristics of eutectoid steel hardened by hydrostatic extrusion are nonmonotonical, and at least two informative testing parameters are needed for nondestructive evaluation of its strength properties, viz., coercive force (or maximum magnetic permeability, residual induction, the number of Barkhausen jumps, the propagation speed of elastic waves) up to the true deformation extent of 1.62 and the root-mean-square voltage of magnetic Barkhausen noises for true deformations above 1.62.

ACKNOWLEDGMENTS

This work was supported by State Order #GR 01201354598 and the Russian Foundation for Basic Research, project no. 16-08-01077. The equipment of Center for Shared Use "Plastometriya" was used in this research.

REFERENCES

1. Safarov, I.M., Korznikov, A.V., Sergeev, S.N., Gladkovskii, S.V., and Borodin, E.M., Effect of submicrocrystalline state on strength and impact toughness of low-carbon 12GBA steel, *Phys. Met. Metallogr.*, 2012, vol. 113, no. 10, pp. 1001–1006.

2. Mavlyutov, A.M., Kasatkin, I.A., Murashkin, M.Yu., Valiev, R.Z., and Orlova, T.S., Influence of the microstructure on the physicomechanical properties of the aluminum alloy Al–Mg–Si nanostructured under severe plastic deformation, *Phys. Solid State*, 2015, vol. 57, no. 10, pp. 2051–2058.
3. Khafizova, E.D., Iskandarova, I.R., Islamgaliev, R.K., and Pankratov, D.L., Structure and mechanical properties of aluminum alloy of the Al-Cu-Mg system after severe plastic deformation, *Pis'ma Mater.*, 2015, vol. 5, no. 4.
4. Ivanov, A.M., Petrova, N.D., and Lepov, V.V., Effect of extrusion and screw compaction on the structure and mechanical properties of low-alloy steel, *Nauka Obraz.*, 2015, no. 4.
5. Gorkunov, E.S., Smirnov, S.V., Zadvorkin, S.M., Grachev, S.V., and Somova, V.M., Kar'kina, L.E., Effect of large deformations during drawing on the physicomechanical properties of patented steel wire, *Phys. Met. Metallogr.*, 2004, vol. 98, no. 5, pp. 521–532.
6. Gorkunov, E.S., Zadvorkin, S.M., Goruleva, L.S., Tueva, E.A., Veselov, I.N., Yakovleva, S.P., Makharova, S.N., and Mordovskoi, P.G., The effect of equal channel angular pressing on the mechanical and magnetic properties of 09G2S steel, *Russ. J. Nondestr. Test.*, 2012, vol. 48, no. 10, pp. 568–575.
7. Beresnev, B.I. and Trushin, E.V., *Protsess gidroekstruzii, (Process of Hydrostatic Extrusion)*, Moscow: Nauka, 1976.
8. Davydova, L.S., Petrov, Yu.N., and Beresnev, B.I., Effect of hydrostatic extrusion on the structure and properties of Armco iron and U8 steel, *Fiz. Met. Metalloved.*, 1977, vol. 43, no. 2, pp. 412–418.
9. Volkov, A.Yu., Antonova, O.V., Kamenetskii, B.I., Klyukin, I.V., Komkova, D.A., and Antonov, B.D., Production, structure, texture, and mechanical properties of severely deformed magnesium, *Phys. Met. Metallogr.*, 2016, vol. 117, no. 5, p. 518–528.
10. Rigmant, M.B., Zinchenko, S.A., Nichipuruk, A.P., Zagainov, A.V., Khudyakov, B.A., and Korkh, M.K., Using magnetic testing to optimize the technology of manufacturing stain-proof austenitic steels, *Russ. J. Nondestr. Test.*, 2016, vol. 52, no. 10, pp. 583–587.
11. Stashkov, A.N., Somova, V.M., Korkh, Yu.V., Ogneva, M.S., Stashkova, L.A., and Sazhina, E.Yu., Magnetic and acoustic techniques for determining the phase composition and destruction dynamics of plastically deformed cobalt-free martensite-aging steel, *Russ. J. Nondestr. Test.*, 2015, vol. 51, no. 7, pp. 433–444.
12. Kostin, V.N., Vasilenko, O.N., Filatenkov, D.Yu., Chekasina, Yu.A., and Serbin, E.D., Magnetic and magnetoacoustic testing parameters of the stressed–strained state of carbon steels that were subjected to a cold plastic deformation and annealing, *Russ. J. Nondestr. Test.*, 2015, vol. 51, no. 10, pp. 624–632.
13. Bakharev, O.G., Gavrilyuk, V.G., Degtyarev, M.V., Levit, V.I., Nadutov, V.M., Svechnikov, V.L., and Chashchukhina, T.I., Effect of hydrostatic extrusion on the structure and phase composition of pearlitic steel, *Fiz. Met. Metalloved.*, 1990, no. 12, pp. 86–90.
14. Bogatov, A.A., Mizhiritskii, O.I., and Smirnov, S.V., *Resurs plastichnosti metallov pri obrabotke davleniem* (Plasticity Life Time of Pressure-Treated Metals), Moscow: Metallurgiya, 1984.
15. Varyukhin, V.N., Pashinskaya, E.G., Zavdoveev, A.V., and Burkhovetskii, V.V., *Vozmozhnosti metoda difraktsii obratnorasseyannykh elektronov dlya analiza struktury deformirovannykh materialov* (Possibilities of Electron Backscattered Diffraction for Analyzing the Structure of Deformed Materials), Kiev: Proekt "Naukova Kniga", 2014.
16. Borodkina, M.M. and Spektor, E.N., *Rentgenograficheskii analiz tekstury metallov i splavov (X-Ray Diffraction Analysis of the Texture of Metals and Alloys)*, Moscow: Metallurgiya, 1981.
17. Gorkunov, E.S., Zadvorkin, S.M., Goruleva, L.S., Makarov, A.V., Pecherkina, N.L., and Cheremitsina, E.R., http://dx.doi. org/. doi 10.1063/1.4967074
18. Schastlivtsev, V.M., Mirzaev, D.A., Yakovleva, I.L., Okishev, K.Yu., Tabatchikova, T.I., and Khlebnikova, Yu.V., *Perlit v uglerodistykh stalyakh (Pearlite in Carbon Steels)*, Yekaterinburg: Ural Branch, Russ. Acad. Sci., 2006.
19. Vitsena, F.O, On the effect of dislocation on the coercive force of ferromagnets, *Cesk. Fiz. Zhurn.*, 1955, vol. 5, no. 4, pp. 480–501.
20. Yensen, T.D. and Ziegler, N.A., Magnetic properties of iron as affected by carbon, oxygen and grain-size, *Trans. Amer. Soc. Met.*, 1935, vol. 23, pp. 556, 557.
21. Kerstern, M., *Grundlagen einer Theorie der ferromagnetischen Hysterese und Koerzitivkraft*, Leipzig: Hirzel, 1943.
22. Vonsovskii, S.V. and Shur, Ya.S., *Ferromagnetizm (Ferromagnetism)*, Moscow: OGIZ, 1948.
23. Kifer, I.I. and Pantyushin, V.S., *Ispytaniya ferromagnitnykh materialov* (Testing of Ferromagnetic Materials), Moscow: Gosenergoizdat, 1955.
24. Hirth, J.P. and Lothe, H., *Theory of Dislocations*, New York: McGraw Hill, Inc., 1982, pp. 764–781.
25. Antolovich, S.D. and Armstrong, R.W., Plastic strain localization in metals: origins and consequences, *Progr. Mater. Sci.*, 2014, vol. 59, pp. 1–160.

Translated by V. Potapchouck